Applied Geochemistry 66 (2016) 234–241

Contents lists available at ScienceDirect

Applied Geochemistry

journal homepage: www.elsevier.com/locate/apgeochem

Diffuse soil gas emissions of gaseous elemental mercury (GEM) from hydrothermal-volcanic systems: An innovative approach by using the static closed-chamber method

F. Tassi [a, b, *], J. Cabassi [a, b], S. Calabrese [c], B. Nisi [d], S. Venturi [a, b], F. Capecchiacci [a, b], L. Giannini [a], O. Vaselli [a, b]

[a] Department of Earth Sciences, University of Florence, Via La Pira 4, Florence 50121, Italy
[b] CNR-IGG Institute of Geosciences and Earth Resources, Via La Pira 4, Florence 50121, Italy
[c] Department of Earth Sciences and Sea, University of Palermo, Via Archirafi 22, Palermo 90123, Italy
[d] CNR-IGG Institute of Geosciences and Earth Resources, Via G. Moruzzi 1, Pisa 56124, Italy

ARTICLE INFO

Article history:
Received 2 November 2015
Received in revised form
7 January 2016
Accepted 9 January 2016
Available online 11 January 2016

Keywords:
GEM flux
Diffuse soil degassing
Air pollutant
Hydrothermal gas

ABSTRACT

This study was aimed to test a new methodological approach to carry out measurements of gaseous elemental mercury (GEM) diffusively emitted from soils in hydrothermal-volcanic environments. This method was based on the use of a static closed-chamber (SCC) in combination with a Lumex® RA-915M analyzer that provides GEM measurements in a wide range of concentrations (from 2 to 50,000 ng m^{-3}). Gas samples were collected at fixed time intervals from the SCC positioned on the ground (time-series samples). The Lumex® inlet port was equipped with a three-way Teflon valve allowing the free entrance of air through a carbon trap, in order to: (i) prevent disturbance to the Lumex® operative flow rate (10 L min^{-1}) during the injection of the gas samples from the SCC and (ii) minimize the instability of the baseline signal induced by possible variations of GEM concentrations in air. In the lab, known amounts of GEM, pipetted from a vessel containing an Hg-saturated air in equilibrium with liquid mercury at 27 °C, were injected in the Lumex® via the modified inlet port to construct a calibration curve. The latter was used to calculate the amount of GEM in the SCC (K_{SCC}) from the corresponding GEM concentrations measured by the Lumex® analyzer. The K_{SCC} values of the time-series samples were proportionally increasing with the GEM fluxes (ϕGEM), thus ϕGEM values were computed according to the following equation: $\phi GEM = (dK_{SCC}/dt)/A$, where A is the basal area of the SCC and dt is the time interval of the time-series sampling. Up to 214 ϕGEM measurements were carried out at Solfatara crater (Campi Flegrei, southern Italy), a hydrothermally altered tuff cone characterized by an anomalous diffuse soil emission of GEM-rich geogenic gases. The measured ϕGEM values varied up to 4 orders of magnitude, from 1,296, corresponding to the sensitivity of the method at the selected sampling time interval (1 min), to 1,957,500 ng m^{-2} day^{-1}, and were consistent with those recently measured in this crater using a different method. In the field, 10 replicates were carried out in 5 selected sites, allowing to demonstrate that the proposed method has a high reproducibility (RDS < 4%). The ϕGEM and ϕCO_2 values, the latter being measured in the same 214 sites by using the accumulation chamber method, showed a low correlation, although both gases were originated from the same deep source. This suggests that GEM and CO_2 soil fluxes are differently affected by environmental parameters, such as soil humidity and temperature, which have a strong effect on the release of GEM from the soil, whereas they do not play a significant role in the diffuse degassing of CO_2. The measured fluxes were used to compute the CO_2 and GEM total outputs (402 and 5.41 × 10^{-6} t day^{-1}, respectively) from the study area (92,000 m^2) and to construct contour maps showing the spatial distribution of the ϕCO_2 and ϕGEM values. By modifying the geometry of SCC and the time interval of the sampling series, the proposed method can be applied to the measurements of GEM soil fluxes in other geological systems and man-made environments.

* Corresponding author. Department of Earth Sciences, University of Florence, Via La Pira 4, Florence 50121, Italy.
E-mail address: franco.tassi@unifi.it (F. Tassi).

http://dx.doi.org/10.1016/j.apgeochem.2016.01.002
0883-2927/

1. Introduction

Mercury is classified as a toxic non-essential heavy metal and it is included among the 189 toxic air pollutants in the Clean Air Act Amendments (CAAA, 1990). The high volatility of this element favors its transport in the atmospheric circulation with a residence time in air of about 0.6 years (Weiss-Penzias et al., 2003). Consequently, a reliable evaluation of the air/surface exchange rates of gaseous elemental mercury (GEM) is critical for estimating its global budget (Rasmussen, 1994; Fitzgerald et al., 1998; Gustin et al., 1999; Pacyna et al., 2006) and developing environmental regulations and controls (WHO, 2007). Notwithstanding, GEM emitted from broad diffuse Hg-enriched soils in natural (e.g. volcanic/hydrothermal systems) and anthropogenic (e.g. landfills, sewage sludge amended soils, mine wastes) environments (e.g., Mason et al., 1994; Boudala et al., 2000; Engle et al., 2001, 2006; Gustin et al., 2002; Marsik et al., 2005; Xin et al., 2006) is difficult to estimate, since the behavior of Hg from these sources is strongly depending on a number of different parameters, such as Hg substrate concentrations, soil temperature and humidity, solar radiation and vegetation cover (e.g., Gustin et al., 2008; Liu et al., 2014, and references therein). Moreover, specific protocols dictating the most appropriate sampling and analytical techniques for GEM flux (ϕGEM) measurements from soils are still matter of debate. In different natural and anthropogenic areas, ϕGEM values have been estimated on the basis of direct measurements carried out with dynamic flux chambers (DFCs) (e.g. Carpi and Lindberg, 1998; Poissant and Casimir, 1998; Stamenkovic and Gustin, 2007; Zhang et al., 2002) or adopting micro-meteorological methods (e.g. Kim et al., 1995; Cobos and Baker, 2002; Edwards et al., 2005; Olofsson et al., 2005; Sommer et al., 2013; Zhu et al., 2015). Systematic experiments were attempted to test the influence of different chamber design/operating conditions and materials on DFC flux measurements (Eckley et al., 2010, and references therein), evidencing that a univocal interpretation to optimize this method is still a challenge. Micrometeorological methods require an accurate selection and estimation of model-based exchange parameters for flux computation and strongly depend on strict meteorological constraints (Zhu et al., 2015, and references therein). Although gas emissions from hydrothermal and volcanic systems are considered to significantly contribute to the Hg global budget, few attempts have been carried out to quantify the atmospheric Hg release from substrates and fumaroles in these natural environments (e.g. Varekamp and Buseck, 1984; Gustin, 2003; Pyle and Mather, 2003; Engle et al., 2006; Aiuppa et al., 2007; Bagnato et al., 2009, 2011, 2013). At Solfatara crater (Campi Flegrei, southern Italy), a tuff cone emitting a huge amount of hydrothermal fluids through both fumarolic vents and diffuse soil degassing (e.g. Chiodini et al., 2005; Aiuppa et al., 2013), a preliminary evaluation of the total budget of GEM was recently carried out by Bagnato et al. (2014). These authors adopted an innovative approach by coupling an accumulation chamber (AC), which has commonly been applied to measure diffuse CO_2 fluxes from soils in volcanic and geothermal areas (e.g. Sorey et al., 1998; Chiodini et al., 1996, 1998, 2001; Gerlach et al., 2001; Cardellini et al., 2003), with a Lumex® RA-915 + analyzer, i.e. a portable Zeeman atomic absorption spectrometer able to measure GEM concentrations, ranging from 2 to 50,000 ng m^{-3} in real-time and at high frequency (1 s). In the present study, a new method for the measurements of GEM fluxes (ϕGEM) diffusively released at the soil-air interface was developed and tested, by using a static closed-chamber (SCC) in combination with a Lumex® RA-915M analyzer. With this aim, on the 4th and 5th of April 2015, a field survey was carried out at Solfatara crater to compare our ϕGEM data with those measured with the AC method. Replicates of ϕGEM measurements in selected sites were also carried out to verify the reproducibility of the proposed procedure. Soil CO_2 fluxes (ϕCO_2) were also determined to investigate the possible relation between the two gases, being both originated from the deep hydrothermal fluid source.

2. Methods and materials

2.1. ϕCO_2 and soil temperature measurements

The ϕCO_2 values were measured at 214 sites within Solfatara crater (Fig. 1) using the AC method. Diffuse degassing in the study area, which belongs to the Campi Flegrei volcanic district (De Vivo et al., 2001), is mainly controlled by NW- and NE-oriented faults and fractures (Chiodini et al., 2001). High-temperature (up to 160 °C) fumaroles are located along the fault system that cuts the southeastern and northeastern walls of the crater (Chiodini et al.,

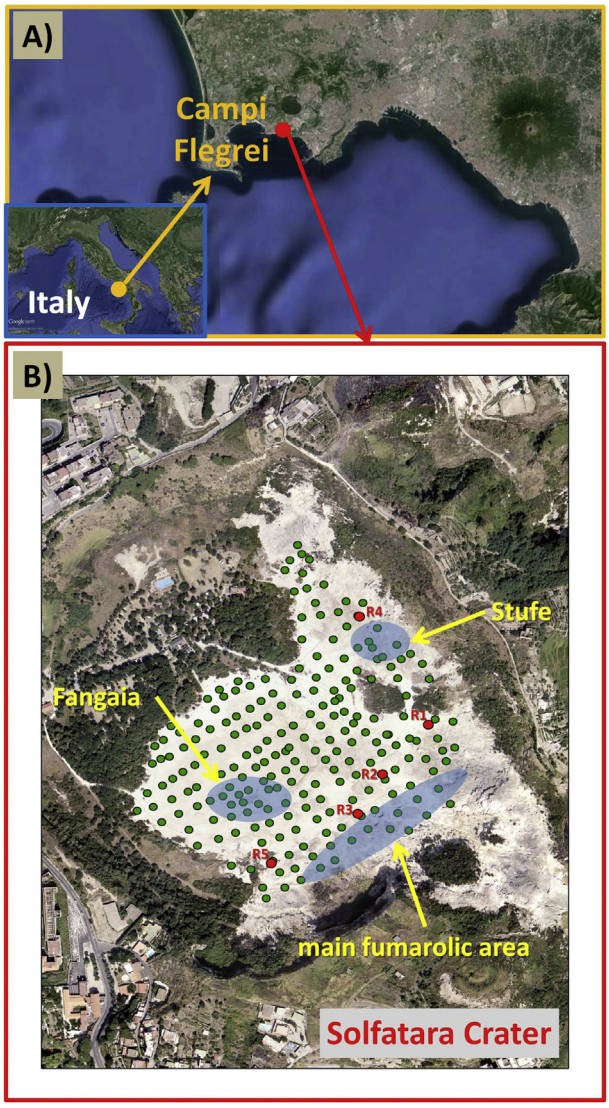

Fig. 1. A) Location of Solfatara crater (Campi Flegrei, southern Italy) and B) distribution of the 214 sites (green circles) where ϕCO_2, ϕGEM and soil temperature measurements were carried out. The red circles indicate the sites selected for the repeated tests used to calculate the reproducibility of the method for the determination of ϕGEM. The blue-colored areas refer to the main degassing sites characterized by fumaroles and bubbling pools (For interpretation of the references to color in this figure legend, the reader is referred to the web version of this article).

2010, Fig. 1). A large area characterized by intense diffuse degassing and the occurrence of mud-pools (*Fangaia*) is hosted in the central part of the crater (Fig. 1). The instrumental apparatus used for the AC measurements consisted of: 1) a metal cylindrical vase (the chamber) with a basal area of 200 cm^2 and an inner volume of 3060 cm^3, 2) an Infra-Red (IR) spectrophotometer (Licor® Li-820). A low-flow pump (20 mL s^{-1}) conveyed the gas from the chamber positioned above the soil to the IR that provided.

continuous CO_2 measurements (up to 20,000 ppm), with an accuracy of 4%. To minimize the disturbance effects due to changes of barometric conditions, the soil gas was re-injected into the chamber. The ϕCO_2 values were computed on the basis of the measured CO_2 concentrations over time ($dC_{CO2}\ dt^{-1}$), using a palmtop computer connected with the IR through an analog-digital (AD) converter and equipped with a Palm Flux 5.36 software, according to the following equation:

$$\phi CO_2 = cf \times dC_{CO2}\ dt^{-1} \quad (1)$$

The proportionality factor (cf) between $dC_{CO2}\ dt^{-1}$ and the ϕCO_2 was determined by measuring ϕCO_2 "standard" values (from 10 to 10,000 g m^{-2} day^{-1}), which were produced using a high-sensitivity flow controller positioned between a stainless cylinder containing pure CO_2 and a "synthetic soil" made of dry sand (10 cm thick) placed inside a plastic box with an open top. At least 6 $dC_{CO2}\ dt^{-1}$ measurements were carried out for each ϕCO_2 standard value. The cf factor was computed as the slope of the linear best-fit line of ϕCO_2 vs. $dC_{CO2}\ dt^{-1}$.

The temperature of the soil at 7 and 15 cm depths was measured using a portable Tersid thermocouple (dynamic range from −20 to 1150 °C; uncertainty ± 0.1 °C).

2.2. ϕGEM measurements

The ϕGEM values were carried out immediately after the ϕCO_2 measurements in the same 214 sites shown in Fig. 1, using a methodological approach that is based on the SCC method (Rolston, 1986; Livingston and Hutchinson, 1995), which has widely been applied for the determination of diffuse CH_4 soil fluxes in geothermal and volcanic environments (e.g., Klusman and LeRoy, 1996; Etiope, 1999; Klusman et al., 2000; D'Alessandro et al., 2009; Castaldi and Tedesco, 2005; Tassi et al., 2013). The SCC used for the present study consisted of an opaque polyethylene cylinder with a basal area of 201 cm^2 and an inner volume of 1810 cm^3. At each measurement point, 4 samples (time-series) were collected from the SCC, i.e. when it was positioned on the ground (time 0; blank value) and after 1, 2 and 3 min. Gas sampling (60 cm^3) from the SCC was carried out by using a syringe equipped with a needle inserted through a pierceable rubber septum positioned on the SCC top (Fig. 2). The removal of the soil gas accumulated in the SCC by the syringe produced a minimal effect on the GEM measurement, being the ratio of the volume of the SCC and that of the syringe of about 30 to 1.

The syringe was then connected to the inlet port of the Lumex® analyzer that was modified by connecting a Teflon three-way valve. One way was equipped with a pierceable rubber septum (the injection inlet), while the third way allowed the free entrance of air through an active carbon trap (Fig. 2), in order to: 1) prevent variations of the operative flow rate of the instrument (10 L min^{-1}) during the injection of the gas samples from the SCC, which could have affected the instrument baseline; 2) minimize the instability of the baseline signal related to the possible occurrence of variable GEM concentrations in air. To calculate the amount of GEM in the syringe (K_{SYR}, in ng), i.e. in 60 cm^3 of sample from the SCC, a calibration curve was constructed using a GEM standard. The latter,

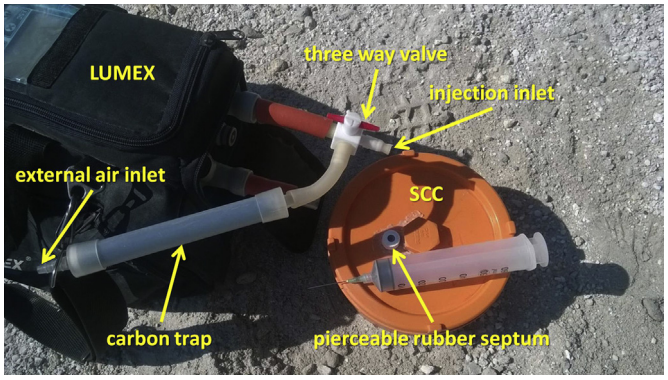

Fig. 2. Injection apparatus of the Lumex® analyzer. The soil gas is collected from SCC through the pierceable rubber septum with a plastic syringe and injected into the Lumex® analyzer through the injection inlet where a Teflon three-way is placed. A carbon trap is connected to the Lumex® analyzer in order to avoid the entrance of external GEM when the instrument is operating (see text for further details).

which was injected with a 500 μL Hamilton gastight micro-syringe through the Lumex® injection port assembled as for the field measurements, was obtained from equilibrated Hg vapor stored in the headspace of a 30 cc vial equipped with a pierceable rubber septum, where liquid Hg was placed and maintained at constant temperature (27 °C). The partial pressure (in atm) of the GEM standard was calculated, as follows (CRC, 2001):

$$P\mathrm{GEM(atm)} = 5.116 + 3190\ T^{-1} \quad (2)$$

where T is in K. At the temperature of the vial (27 °C), *P*GEM was thus equal to 3.076×10^{-6} atm, corresponding to 0.02804 ng μL^{-1} of GEM. As reported in Table 1, 8 different aliquots (from 20 to 300 μL) of the GEM standard (corresponding to 0.56–8.41 ng of GEM) were repeatedly injected (10 times) in the Lumex® analyzer. The GEM concentrations (in ng m^{-3}), i.e. the maximum value of the peak measured by the instrument after each standard injection, were used to calculate (i) the relative standard deviation (RSD ≤ 4%; Table 1) and (ii) the average values (Table 1) for each standard series. The 8 average values of the GEM standard plot on a polynomial curve ($y = 5 \times 10^{-8}x^2 + 0.0006x$), i.e. the calibration curve (Fig. 3), with r^2 up to 0.99, a value that is statistically significant since, according to the F-test, the p-value is <<0.01. By an operative point of

Table 1
GEM concentrations (ng m^{-3}) for repeated (10 replicates) measurements of 8 aliquots (20, 50, 75, 100, 150, 200, 250 and 300 μL; the corresponding GEM quantities, in ng, were also reported) of GEM standard. The relative standard deviation (RDS, in %), average and median values (ng m^{-3}) for each standard series are also reported.

μL	20	50	75	100	150	200	250	300
ng	0.56	1.40	2.10	2.80	4.21	5.61	7.01	8.41
Replicates								
1	802	1930	2810	3414	4851	6000	7000	7935
2	780	1820	2657	3494	4658	6020	6819	7882
3	771	1939	2849	3461	4645	6113	7038	8021
4	815	1779	2783	3481	4592	6144	6971	8075
5	831	1934	2773	3527	4803	6003	7021	7906
6	822	1795	2780	3439	4846	6001	6959	7904
7	824	1882	2799	3492	4546	6013	6796	7969
8	777	1924	2812	3535	4905	6107	7047	8095
9	743	1803	2830	3548	4823	6054	6922	8041
10	739	1836	2782	3422	4850	6152	7010	8092
average	790	1864	2788	3481	4752	6061	6958	7992
median	791	1859	2791	3487	4813	6037	6986	7995
RSD	4.0	3.3	1.8	1.3	2.6	1.0	1.2	1.0

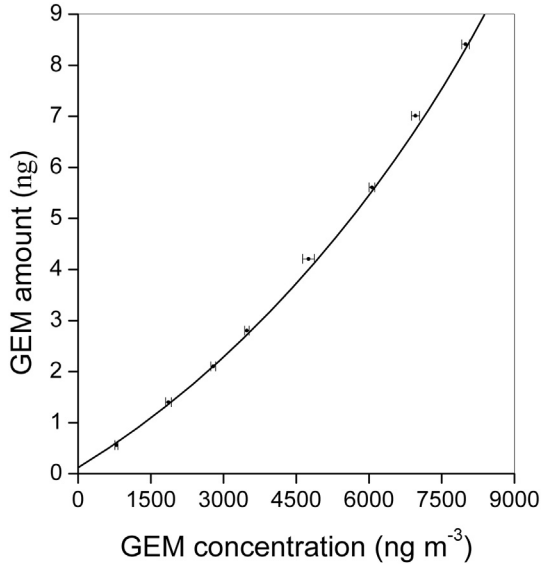

Fig. 3. Calibration curve for GEM concentrations (in ng m^{-3}) measured by the Lumex® analyzer equipped with the injection port apparatus on the basis of known GEM amounts (in ng). The error bar (RDS %) for each repeated standard series is also plotted.

view, the K_{SYR} value of each injection was calculated by interpolating in the calibration curve the corresponding GEM concentrations provided by the Lumex analyzer. The GEM amount in the SCC (K_{SCC}, in ng) was computed by multiplying the K_{SYR} values for the ratio between the volume of the gas injected from the syringe (60 cm^3) and that of the SCC (1810 cm^3). For each time-series, the K_{SCC} blank value (i.e. that measured when the chamber was positioned on the ground) was subtracted to those measured after 1, 2 and 3 min. The three resulting K_{SCC} values were used to compute the ϕGEM values (in ng m^{-2} day^{-1}), according to the general equation relating the increase of a X gas species in the SCC and the ϕX values, as follows:

$$\phi GEM = (dK_{SCC}/dt)/A \quad (3)$$

where A is the basal area of the SCC and dt is the time sampling interval (1 min).

3. Results and discussion

3.1. ϕCO_2 values and soil temperatures

The ϕCO_2 values were from 19.8 to 118,000 g m^{-2} day^{-1}, whereas the average and median values were 4578 and 1321 g m^{-2} day^{-1}, respectively. Such a wide range, more than 4 orders of magnitude, is a typical feature for ϕCO_2 at Solfatara crater, where fumarolic vents occur and the diffuse release of hydrothermal CO_2-rich gases from the crater soil is favored by a complex system of fractures (e.g. Todesco et al., 2003). The occurrence of fractures, where measurement points showed extremely high fluxes, caused the strongly asymmetrical distribution of the ϕCO_2 data (average >> median). The maximum soil temperatures at 7 and 15 cm depths were the relatively high (both up to 95 °C), being related to heat convectively transported from the hydrothermal system by the uprising fluids. Evidences of a thermal gradient occurring in the crater soil were also provided by (i) the significant increase with depth of both the average and median temperatures (from 31.3 to 39.5 °C and from 25.5 to 32.0 °C, respectively) and (ii) the strong correlation ($r^2 = 0.92$; p-value <<0.01) between the soil temperatures measured at the two different depths (Fig. 4a). Surprisingly, ϕCO_2 and soil temperatures (Fig. 4b) show a low correlation ($r^2 = 0.21$; p-value <<0.01). It has to be considered that convective heat is mostly associated with water vapor, since gases, including CO_2, have a low thermal capacity. With the exception of the fumarolized zones (Fig. 1), the temperature of the crater soil was below that of boiling water, thus the uprising hydrothermal fluids were likely affected by a significant condensation process, which possibly explains the decoupling between ϕCO_2 and soil temperature.

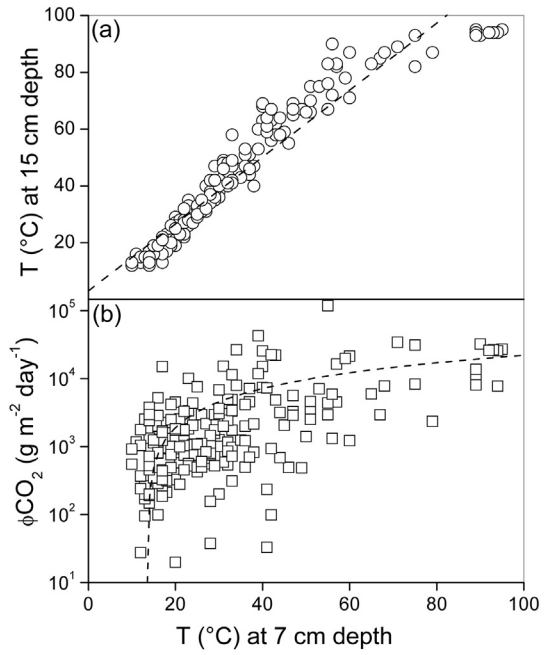

Fig. 4. Soil temperature (T °C) at 7 cm depth vs. (a) T (°C) at 15 cm depth and (b) ϕCO_2 (g m^{-2} day^{-1}) binary diagrams measured at Solfatara crater.

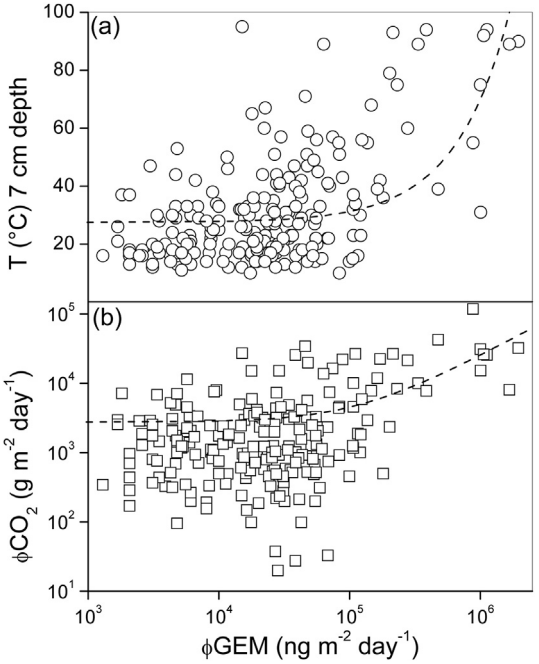

Fig. 5. ϕGEM (ng m^{-2} day^{-1}) vs. (a) (T °C) at 7 cm depth and (b) ϕCO_2 (g m^{-2} day^{-1}) binary diagrams measured at Solfatara crater.

Table 2
Replicated (10 times) ϕGEM measurements (ng m^{-2} d^{-1}) carried out at 5 selected sites (Fig. 1) at Solfatara crater for the reproducibility test. For each repeated series, RDS (%), average and median values (ng m^{-2} d^{-1}) are also reported.

Replicates	R1	R2	R3	R4	R5
1	17,945	11,690	20,819	271,431	50,639
2	17,556	13,383	22,126	289,328	53,282
3	17,294	13,253	20,427	281,337	53,812
4	18,338	13,383	21,211	274,161	51,833
5	18,991	12,731	22,126	278,997	55,799
6	17,816	13,513	21,603	281,284	56,196
7	18,208	12,993	20,689	281,592	53,545
8	18,729	13,904	20,689	280,605	55,795
9	18,729	13,904	21,734	271,227	51,563
10	18,599	13,122	21,733	292,349	56,328
average	18,221	13,188	21,316	280,231	53,879
median	18,273	13,318	21,407	280,944	53,678
RSD	2.9	4.6	2.8	2.3	3.7

3.2. ϕGEM values

The ϕGEM values, similarly to those of ϕCO_2, were varying in a wide range (from 1296 to 1,957,500 ng m^{-2} day^{-1}) and the difference between the average and median values (85,680 and 22,390 ng m^{-2} day^{-1}, respectively) highlights an asymmetrical distribution of the measured data, i.e. the occurrence of relatively few, anomalously high ϕGEM values (Table 1A in the Supplementary Material), whose occurrence was likely not related to any temporal change of the deep emitting source, considering that all the 214 measurements were carried out in a relatively short time (less than 30 h). Therefore, the local fracture system, which typically controls the ϕCO_2 and soil temperature values, played an important role also for the GEM diffuse degassing. The minimum ϕGEM value (1296 ng m^{-2} day^{-1}), corresponding to an increase of 1 ng m^{-3} min^{-1} in the SCC, was dictated by the sensitivity of the Lumex® analyzer (1 ng m^{-3}). However, this detection limit, which depends on the selected time-interval of the sampling series and the dimension of the SCC, was adequate to measure ϕGEM in all the selected points of the study area.

It is worth to mention that the ϕGEM values were poorly correlated to both soil temperatures (r^2 = 0.29; p-value <<0.01) and those of ϕCO_2, (r^2 = 0.28; p-value <<0.01) (Fig. 5a and b, respectively). Although consistent with previous data (r^2 = 0.35; Bagnato et al., 2014), a low correlation between the ϕCO_2 and ϕGEM values was unexpected, since both CO_2 and GEM in the Solfatara crater emission are clearly associated with the same deep hydrothermal source. On the contrary, flux values of other deep-originated gaseous compounds discharged from the Solfatara soil, such as C_6H_6, whose chemical behavior is similar to that of CO_2, were found in close association with those of ϕCO_2 (Tassi et al., 2013). The disagreement between the ϕGEM and ϕCO_2 data was likely depending on a number of environmental parameters, such as soil humidity and temperature, which typically affect the release of GEM from the soil (e.g., Gustin and Stamenkovic, 2005), whereas their effect on soil diffuse CO_2 degassing is not significant. The permanent acidic aquifer occurring at shallow depth below the Solfatara crater (Tassi et al., 2013) may also significantly contribute

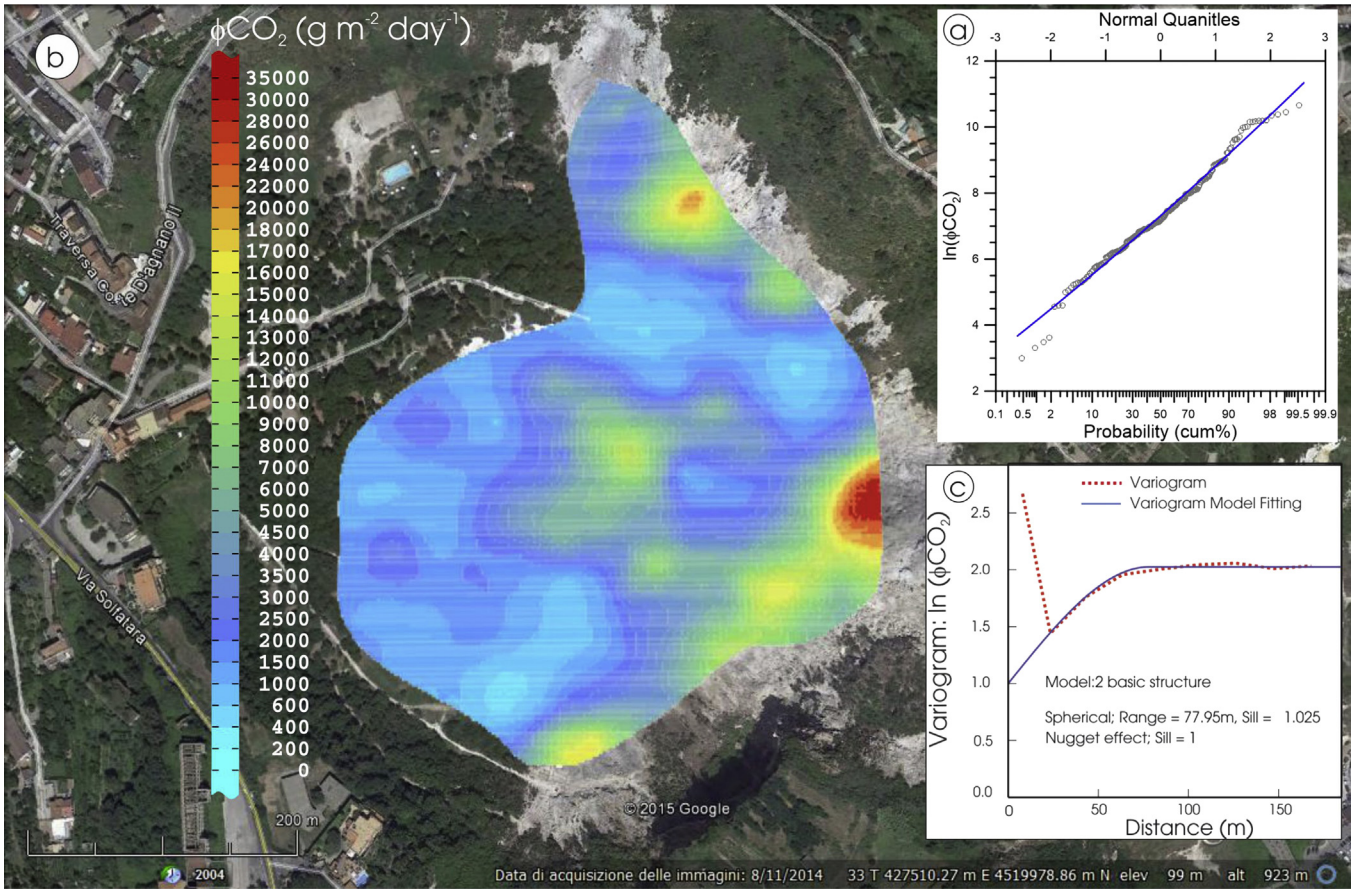

Fig. 6. (A) Probability plot of ln(ϕCO_2) (g m^{-2} day^{-1}) constructed by applying the partitioning method of Sinclair (1974, 1991). Solid lines represent the theoretical distribution. (B) Contour map of ϕCO_2 from the soil of Solfatara crater. (C) Variogram and model fitting of ln(ϕCO_2).

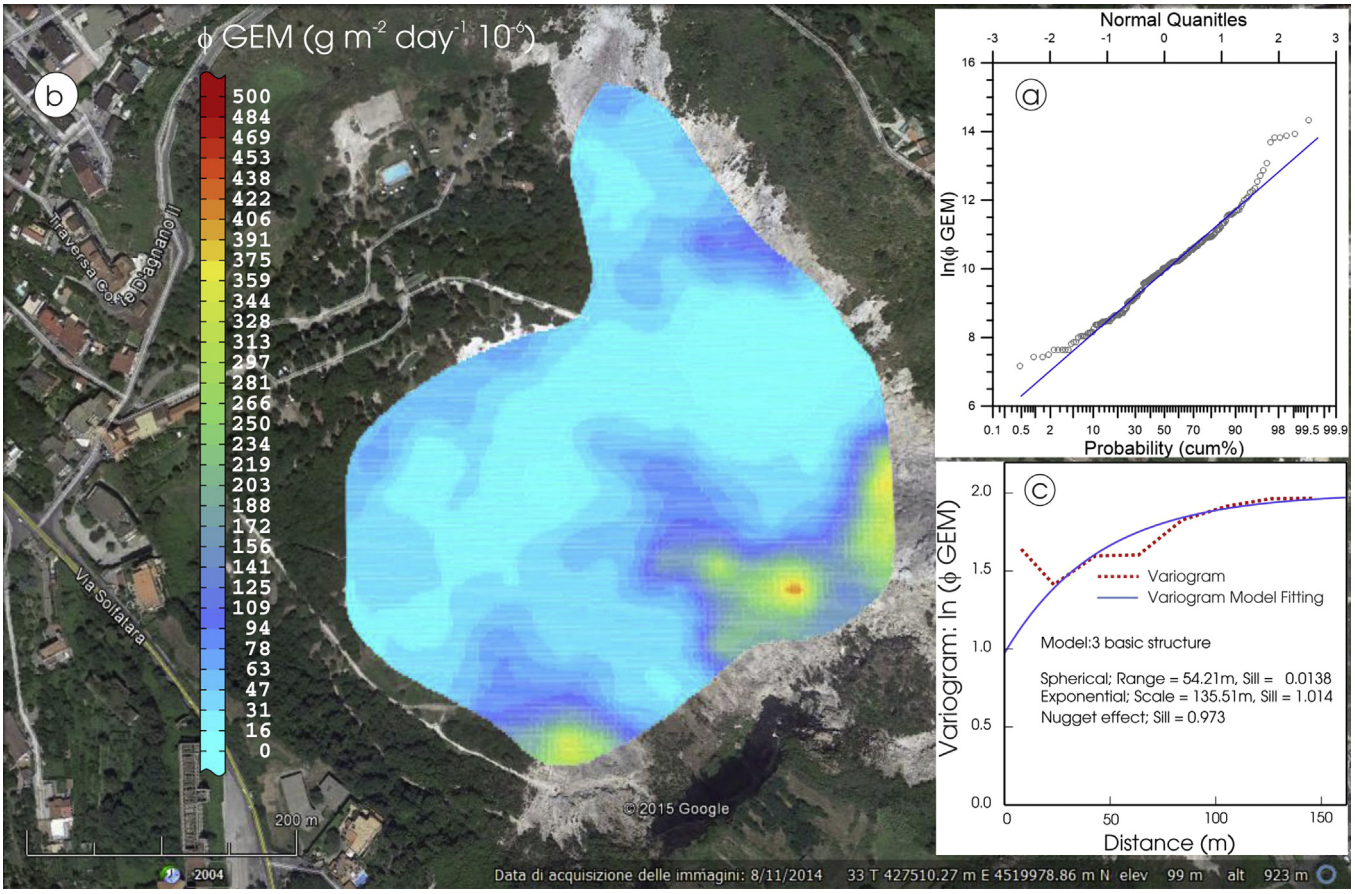

Fig. 7. (A) Probability plot of ln(ϕGEM) (ng m^{-2} day^{-1}) constructed as in Fig. 6a. (B) Contour map of ϕGEM from the soil of Solfatara crater. (C) Variogram and model fitting of ln(ϕGEM).

to scrub GEM from the uprising gases.

3.3. Reproducibility test

To evaluate the reproducibility of the method, 10 replicates of ϕGEM measurements were carried out at 5 selected sites at Solfatara crater (R1 to R5 in Fig. 1), with the same (SCC + Lumex®) equipment and method used for the spatial survey. The time interval between the replicates was <1 min. Once a replicate series at a site was completed, we moved to the next reproducibility test site. The ϕGEM average values were from 13,188 (R2) to 280,231 (R4) ng m^{-2} day^{-1} (Table 2), i.e. consistent with most of the 214 ϕGEM values measured in the crater floor (Table 1A). The RDS values of the test data series (from 2.3 to 4.6%; Table 3) were relatively low and in the range of those calculated for the standard measurements (Table 1). This suggests that the field operations with the SCC, independently on the ϕGEM values, had no significant effects on the reproducibility of the method. Moreover, the replicates carried out in the 5 sites do not show any trend and their distribution is symmetrical (average and median values are almost coincident; Table 2), thus excluding that the reproducibility test measurements were affected by a memory effect.

3.4. Total ϕCO_2 and ϕGEM output and spatial distribution maps

To estimate the total amount of the CO_2 and GEM fluxes released from Solfatara crater, the measured flux data were processed using a classical graphical-statistical approach (Sinclair, 1974, 1991). The probability plot (Fig. 6a and Fig. 7a) suggested that the ln(ϕCO_2) and ln(ϕGEM) values have a single ln-normal population. According to the Sichel's t estimator (David, 1977), the total diffuse CO_2 output at the Solfatara crater is 402 t day^{-1}, whereas that of GEM is $5.41 \bullet 10^{-6}$ t day^{-1}, i.e. consistent with the estimations carried out by Bagnato et al. (2014). The upper and lower limits at 95% confidence are 578 and 305 t day^{-1} (CO_2) and $7.82 \bullet 10^{-6}$ and $4.21 \bullet 10^{-6}$ t day^{-1} (GEM), respectively.

The CO_2 and (GEM) iso-flux maps, reported in Figs. 6b and 7b, respectively, were constructed by applying geostatistical methods (e.g. Krige, 1951; Matheron, 1970). The data processing indicates that the combination of two (Spherical model with a nugget effect, Fig. 6c) and three (Exponential and Spherical models with a nugget effect, Fig 7c) basic structures is the best approach to describe the spatial variability of the ϕCO_2 and ϕGEM values, respectively. The contour map of the ϕGEM values (Fig. 7b) highlights the strong anomaly occurring in the SE part of the crater, where the fumarolic vents, discharging a visible plume of hydrothermal vapors, are located. It is worth noting that the ϕGEM spatial distribution roughly resembles that of ϕCO_2 (Fig. 6b), although the ϕGEM and ϕCO_2 values showed a poor correlation (Fig. 5b). This suggests that the graphical representations smooth the discrepancies shown by the fluxes of the two compounds related to their different chemical-physical behavior.

4. Conclusions

This study demonstrated that ϕGEM from the soil in hydrothermal systems can reliably be measured by coupling the SCC technique with a Lumex® analyzer. The proposed method was

applied at Solfatara crater, where ϕGEM measurements were carried out at 214 sites and compared with those of ϕCO_2, the latter being commonly used for the geochemical monitoring of this active volcanic system (Chiodini et al., 2010). Although the origin of both CO_2 and Hg is related to the uprising of the hydrothermal fluids, the ϕGEM and ϕCO_2 values showed a low correlation, likely due to scrubbing processes affecting GEM at relatively shallow depth. A specific test carried out in the study area demonstrated that the SCC-Lumex® method has a satisfactory reproducibility (<4%) in a wide range of ϕGEM values.

The proposed methodological approach unequivocally has some advantages with respect to the micrometeorological and DFC methods: 1) the analytical equipment, including the injection apparatus set at the Lumex® inlet port, can be calibrated with external standards; 2) field operations are rapid and they do not require a prolonged exposure of the instrument to aggressive gases typically occurring in a hydrothermal/volcanic environment; 3) besides GEM, different gas species (e.g. CH_4, light hydrocarbons, NO_x) can be collected from the SCC sampled, allowing the simultaneous measurement of their fluxes (e.g. Tassi et al., 2013); 4) the total GEM output from areas characterized by anomalous gas emissions can be computed on the basis of a statistically significant number of measurements and, in combination with the budget of other deep-originated gases, used for the geochemical monitoring of active volcanic system. Although the amount of GEM diffusively discharged from Solfatara crater likely has a limited environmental impact with respect to that related to the release in air of the main hydrothermal compounds (e.g. CO_2, CH_4, H_2S, C_6H_6), the development and application of this method in different hydrothermal areas can significantly contribute to improve the estimation of the global GEM budget.

It is worth noting that the ϕGEM values commonly measured by using other methodological approaches in areas not affected by hydrothermal fluid emissions (e.g. Zhu et al., 2015, and references therein) are significantly lower with respect to those measured at Solfatara crater. Nevertheless, by lowering the V/A ratio of the chamber and/or increasing the time interval of the sampling series, the SCC sensitivity can easily be improved, allowing the measurement of ϕGEM in different natural and anthropogenic systems.

Acknowledgments

This work was supported by the V2-INGV-DPC Project, the Municipality of Abbadia San Salvatore (Siena, Itay) and the laboratories of Fluid Geochemistry and Stable Isotopes of the Department of Earth Sciences of the University of Florence. Many thanks are due to three anonymous reviewers and the Editor for their comments that improved an early version of the manuscript. A. Buccianti is warmly thanked for her useful statistical suggestions on the data processing of the calibration curve.

Appendix A. Supplementary data

Supplementary data related to this article can be found at http://dx.doi.org/10.1016/j.apgeochem.2016.01.002.

References

Aiuppa, A., Bagnato, E., Witt, M.L.I., Mather, T.A., Parello, F., Pyle, D.M., Martin, R.S., 2007. Real-time simultaneous detection of volcanic Hg and SO2 at La Fossa crater, Vulcano (Aeolian Islands, Sicily). Geophys. Res. Lett. 34, L21307. http://dx.doi.org/10.1029/2007GL030762.

Aiuppa, A., Tamburello, G., Di Napoli, R., Cardellini, C., Chiodini, G., Giudice, G., Grassa, F., Pedone, M., 2013. First observations of the fumarolic gas output from a restless caldera: Implications for the current period of unrest (2005–2013) at Campi Flegrei. Geochem. Geophys. Geosyst. 14, 4153–4169. http://dx.doi.org/10.1002/ggge.20261.

Bagnato, E., Allard, P., Parello, F., Aiuppa, A., Calabrese, S., Hammouya, G., 2009. Mercury gas emissions from La Soufrière volcano, Guadeloupe island (Lesser Antilles). Chem. Geol. 266, 276–282.

Bagnato, E., Aiuppa, A., Parello, F., Allard, P., Liuzzo, M., Giudice, G., Shinohara, H., 2011. New clues on mercury contribution from earth volcanism. Bull. Volcanol. 73, 497–510. http://dx.doi.org/10.1007/s00445-010-0419-y.

Bagnato, E., Tamburello, G., Aiuppa, A., Sprovieri, M., Vougioukalakis, G.E., Parks, 2013. Atmospheric mercury emissions from substrate and fumaroles at Nea Kameni volcanic system, Santorini (Greece). Geochem. J. 47 (4), 437–450.

Bagnato, E., Barra, M., Cardellini, C., Chiodini, G., Parello, F., Sprovieri, M., 2014. First combined flux chamber survey of mercury and CO_2 emissions from soil diffuse degassing at Solfatara of Pozzuoli crater, Campi Flegrei (Italy): mapping and quantification of gas release. J. Volcanol. Geotherm. Res. 289, 26–40.

Boudala, F.S., Folkins, I., Beauchamp, S., Tordon, R., Neima, J., Johnson, B., 2000. Mercury flux measurements over air and water in Kejimkujik National Park, Nova Scotia. Water Air Soil Poll. 122, 183–202.

CAAA, 1990. Clean Air Act Amendments. United States Environmental Protection Agency. http://www.epa.gov/air/caa/.

Cardellini, C., Chiodini, G., Frondini, G., 2003. Application of stochastic simulation to CO_2 flux from soil: mapping and quantification of gas release. J. Geophys. Res. 108, 2425. http://dx.doi.org/10.1029/2002JB002165.

Carpi, A., Lindberg, S.E., 1998. Application of a teflon (TM) dynamic flux chamber for quantifying soil mercury flux: tests and results over background soil. Atmos. Environ. 32, 873–882.

Castaldi, S., Tedesco, D., 2005. Methane production and consumption in an active volcanic environment of Southern Italy. Chemosphere 58, 131–139.

Chiodini, G., Frondini, F., Raco, B., 1996. Diffuse emission of CO_2 from the Fossa crater. Vulcano Isl. Bull. Volcanol. 58, 41–50.

Chiodini, G., Cioni, R., Guidi, M., Raco, B., Marini, L., 1998. Soil CO_2 flux measurements in volcanic and geothermal areas. Appl. Geochem 13, 543–552.

Chiodini, G., Frondini, F., Cardellini, C., Granieri, D., Marini, L., Ventura, G., 2001. CO_2 degassing and energy release at Solfatara volcano, Campi Flegrei, Italy. J. Geophys. Res. 106, 16213–16221. http://dx.doi.org/10.1029/2001JB000246.

Chiodini, G., Granieri, D., Avino, R., Caliro, S., Costa, A., Werner, C., 2005. Carbon dioxide diffuse degassing and estimation of heat release from volcanic and hydrothermal systems. J. Geophys. Res. 110, B08204. http://dx.doi.org/10.1029/2004JB003542.

Chiodini, G., Caliro, S., Cardellini, C., Granieri, D., Avino, R., Baldini, A., Donnini, M., Minopoli, C., 2010. Long-term variations of the Campi Flegrei, Italy, volcanic system as revealed by the monitoring of hydrothermal activity. J. Geophys. Res. 115, B03205. http://dx.doi.org/10.1029/2008JB006258.

Cobos, D.R., Baker, J.M., 2002. Conditional sampling for measuring mercury vapor fluxes. Atmos. Environ. 36, 4309–4321.

CRC, 2001. In: Lide, D.R. (Ed.), Handbook of Chemistry and Physics, 82nd ed. CRC Press, Boca Raton, FL, USA.

D'Alessandro, W., Bellomo, S., Brusca, L., Fiebig, J., Longo, M., Martelli, M., Pecoraino, G., Salerno, F., 2009. Hydrothermal methane fluxes from the soil at Pantelleria island (Italy). J. Volcanol. Geotherm. Res. 187, 147–157.

De Vivo, B., Rolandi, G., Gans, P.B., Calvert, A., Bohrson, W.A., Spera, F.J., Belkin, H.E., 2001. New constraints on the pyroclastic eruptive history of the Campanian Volcanic Plain (Italy). Mineral. Petrol 73, 47–65.

Eckley, C.S., Gustin, M., Lin, C.-J., Li, X., Miller, M.B., 2010. The influence of dynamic chamber design and operating parameters on calculated surface-to-air mercury fluxes. Atmos. Environ. 44, 194–203.

Edwards, G.C., Rasmussen, P.E., Schroeder, W.H., Wallace, D.M., Halfpenny-Mitchell, L., Dias, G.M., Kemp, R.J., Ausma, S., 2005. Development and evaluation of a sampling system to determine gaseous mercury fluxes using an aerodynamic micrometeorological gradient method. J. Geophys. Res.-Atmos. 110, D10306.

Engle, M.A., Gustin, M.S., Zhang, H., 2001. Quantifying natural source mercury emissions from the Ivanhoe Mining District, north-central Nevada, USA. Atmos. Environ. 35, 3987–3997.

Engle, M.A., Gustin, M.S., Goff, F., Counce, D.A., Janik, C.J., Bergfeld, D., Rytuba, J.J., 2006. Atmospheric mercury emissions from substrates and fumaroles associated with three hydrothermal systems in the western United States. J. Geophys. Res. 111, D17304.

Etiope, G., 1999. Subsoil CO_2 and CH_4 and their advective transfer from faulted grassland to the atmosphere. J. Geophys. Res. 104D, 16889–16894. http://dx.doi.org/10.1029/1999JD900299.

Fitzgerald, W.F., Engstrom, D.R., Mason, R.P., Nater, E.A., 1998. The case for atmospheric mercury contamination in remote areas. Environ. Sci. Technol. 32, 1–7.

Gerlach, T.M., Doukas, M.P., McGee, K.A., Klesser, R., 2001. Soil efflux and total emission rates of magmatic CO_2 at the Horseshoe Lake tree kill, Mammoth Mountain California, 1995–1999. Chem. Geol. 177, 85–99.

Gustin, M.S., 2003. Are mercury emissions from geologic sources significant? A status report. Sci. Total Environ. 304, 153–167.

Gustin, M., Lindberg, S., Marsik, F., Casimir, A., Ebinghaus, R., Edwards, G., Fitzgerald-Hubble, C., Kemp, R., Kock, H., Leonard, T., London, J., Majewski, M., Owens, J., Pilote, M., Poissant, L., Rasmussen, P., Schaedlich, F., Schneeberger, D., Schroeder, W., Sommar, J., Turner, R., Vette, A., Walschlaeger, D., Xiao, Z., Montecinos, C., Zhang, H., 1999. The Nevada SToRMS project: measurement of mercury emissions from naturally enriched surfaces. J. Geophys. Res. 104, 21831–21844.

Gustin, M.S., Biester, H., Kim, C.S., 2002. Investigation of the light-enhanced emission of mercury from naturally enriched substrates. Atmos. Environ. 36,

3241–3254.
Gustin, M.S., Stamenkovic, J., 2005. Mercury emissions from soils: effect of watering and soil water content. Biogeochem 76, 215–232.
Gustin, M.S., Kolker, A., Gardfeldt, K., 2008. Transport and fate of mercury in the environment. Appl. Geochem 23, 343–344.
Kim, K.H., Lindberg, S.E., Meyers, T.P., 1995. Micrometeorological measurements of mercury-vapor fluxes over background forest soils in Eastern Tennessee. Atmos. Environ. 29, 267–282.
Klusman, R.W., LeRoy, M.P., 1996. Potential for use of gas ux measurements in surface exploration for geothermal resources. Geoth. Resour. Counc. Trans. 20, 331–338.
Klusman, R.W., Moore, J.N., LeRoy, M.P., 2000. Potential for surface gas flux measurements in exploration and surface evaluation of geothermal resources. Geothermics 29, 637–670.
Krige, D.G., 1951. A statistical approach to some basic mine valuation problems on the Witwatersrand. J. Chem. Metall. Min. Soc. S. Afr. 52, 119–139.
Liu, F., Cheng, H., Yang, K., Zhao, C., Liu, Y., Peng, M., Li, K., 2014. Characteristics and influencing factors of mercury exchange flux between soil and air in Guangzhou City. J. Geochem. Expl. 139, 115–121.
Livingston, G.P., Hutchinson, G.L., 1995. Enclosure-based measurement of trace gas exchange: applications and sources of error. In: Matson, P.A., Harris, R.C. (Eds.), Biogenic Trace Gases: Measuring Emissions from Soil and Water. Methods in Ecology. Blackwell Science Cambridge University Press, London, pp. 14–51.
Marsik, F.J., Keeler, G.J., Lindberg, S.E., Zhang, H., 2005. Air-surface exchange of gaseous mercury over a mixed sawgrass-cattail stand within the Florida Everglades. Environ. Sci. Technol. 39, 4739–4746.
Mason, R.P., Fitzgerald, W.F., Morel, F.M.M., 1994. The biogeochemical cycling of elemental mercury: anthropogenic influences. Geochim. Cosmochim. Acta 58, 3191–3198.
Matheron, G., 1970. The theory of regionalized variables and its applications. Fascicule n. 5, Les Cahiers du Centre De Morphologie Mathématique, École des Mines de Paris, Fontainebleau, p. 211.
Olofsson, M., Sommar, J., Ljungström, E., Andersson, M., 2005. Application of relaxed eddy accumulation techniques to qualify Hg0 fluxes over modified soil surfaces. Water Air Soil Poll. 167, 331–354.
Pacyna, E.G., Pacyna, J.M., Steenhuisen, F., Wilson, S., 2006. Global anthropogenic mercury emission inventory for 2000. Atmos. Environ. 40, 4048–4063.
Poissant, L., Casimir, A., 1998. Water-air and soil-air exchange rate of total gaseous mercury measured at background sites. Atmos. Environ. 32, 883–893.
Pyle, D.M., Mather, T.A., 2003. The importance of volcanic emissions for the global atmospheric mercury cycle. Atmos. Environ. 3, 5115–5124.
Rasmussen, P.E., 1994. Current methods of estimating atmospheric mercury fluxes in remote areas. Environ. Sci. Technol. 28, 2233–2241.
Rolston, D.E., 1986. Gas flux. In: Klute, A. (Ed.), Methods of Soil Analysis. Part1. Physical and Mineralogical Methods, second ed. ASA, Madison, WI, pp. 1103–1119.
Sinclair, A.J., 1974. Selection of thresholds in geochemical data using probability graphs. J. Geochem. Expl. 3, 129–149.
Sinclair, A.J., 1991. A fundamental approach to threshold estimation in exploration geochemistry: probability plots revisited. J. Geochem. Expl. 41, 1–22.
Sorey, M.L., Evans, W.C., Kennedy, C.D., Farrar, C.D., 1998. Carbon dioxide and helium emissions from a reservoir of magmatic gas beneath Mammoth Mountain, California. J. Gephys. Res. 103, 15303–15323.
Stamenkovic, J., Gustin, M.S., 2007. Evaluation of use of eco- cell technology for quantifying total gaseous mercury fluxes over background substrates. Atmos. Environ. 41, 3702–3712.
Tassi, F., Nisi, B., Cardellini, C., Capecchiacci, F., Donnini, M., Vaselli, O., Avino, R., Chiodini, G., 2013. Diffuse soil emission of hydrothermal gases (CO_2, CH_4, and C_6H_6) at Solfatara crater (Campi Flegrei, southern Italy). Appl. Geochem 35, 142–153.
Todesco, M., Chiodini, G., Macedonio, G., 2003. Monitoring and modelling hydrothermal fluid emission at La Solfatara (Phlegrean Fields, Italy). An interdisciplinary approach to the study of diffuse degassing. J. Volcanol. Geotherm. Res. 125, 57–79.
Varekamp, J.C., Buseck, P.R., 1984. The speciation of Hg in hydrothermal systems, with applications for ore deposition. Geochim. Cosmochim. Acta 48, 177–185.
Weiss-Penzias, P., Jaffe, D., McClintick, A., Prestbo, E.M., Landis, M.S., 2003. Gaseous elemental mercury in the marine boundary layer: evidence for rapid removal in anthropogenic pollution. Environ. Sci. Technol. 37, 3755–3763.
WHO, 2007. Exposure to Mercury: a Major Public Health Concern. World Health Organization and United Nations Environment Programme, Geneva, Switzerland.
Xin, M., Gustin, M.S., Ladwig, K., Pflughoeft-Hassett, D.F., 2006. Air-substrate mercury exchange associated with landfill disposal of coal combustion products. J. Air Waste Manag. Ass 56, 1167–1176.
Zhang, H., Lindberg, S.E., Barnett, M.O., Vette, A.F., Gustin, M.S., 2002. Dynamic flux chamber measurement of gaseous mercury emission fluxes over soils. Part 1: simulation of gaseous mercury emissions from soils using a two-resistance exchange interface model. Atmos. Environ. 36, 835–846.
Zhu, W., Sommar, J., Feng, X., 2015. Mercury vapor air-surface exchange measured by collocated micrometeorological and enclosure methods – Part I: data comparability and method characteristics. Atmos. Chem. Phys. 15, 685–702.